

Computational approach proposition for further processing of the fatigue curve

M. Sága^{a,*}, M. Vaňko^a, M. Malcho^a, J. Jandačka^a

^a Faculty of Mechanical Engineering, University of Āilina, Univerzitn 1, 010 26 Āilina, Slovakia

Received 7 September 2007; received in revised form 10 October 2007

Abstract

The goal of our paper is to present the numerical computational tools application for the hysteretic curve identification using Karray-Bouc and Ramberg-Osgood models. The Karray-Bouc model parameters will be determined from Ramberg-Osgood model and Manson-Coffin curve parameters. Using special Matlab[®] procedures we can calculate dissipative (hysteretic) energy density per cycle and express Manson-Coffin curve in energy version.

© 2007 University of West Bohemia. All rights reserved.

Keywords: Manson-Coffin curve, energy fatigue curve, Karray-Bouc hysteretic model, Ramberg-Osgood model

1. Introduction

The engineering structures components usually undergo a non-proportional and multiaxial loading. The application of the cyclic σ - ε tensor response under the multiaxial loading, which depends on the loading-path, is very difficult [12,2]. Several researchers have proposed uniaxial and multiaxial fatigue criteria based on an energy evaluation [8,10,6]. Hence, the goal of the paper will be to present possibilities how to determine the energy-based fatigue curve from Manson-Coffin curve [7,10,6,15].

Considering low and high cyclic fatigue life it will be needed to express the cyclic σ - ε curve mathematically. The hysteretic models can be continuous and discontinuous (e.g. linear in parts). The behaviour σ - ε can have a monotonic character or a cyclic character (Fig. 1) [3,12,15].

The first models have been described by simple algebraic equations mainly for the monotonic σ - ε relationship. Further, we will use one of the first models with the exponential character of hardening known as Ramberg-Osgood model (RO), i.e.

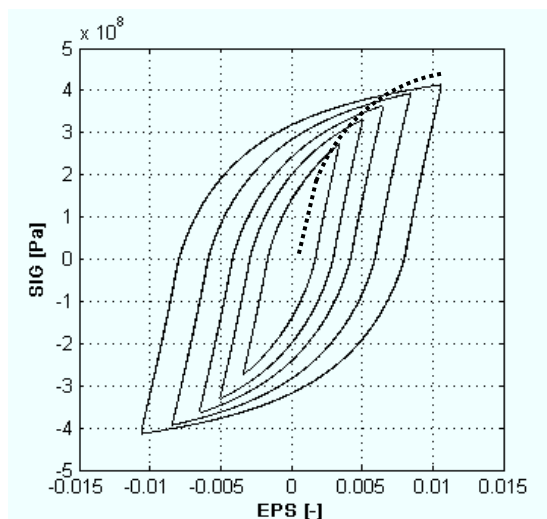


Fig. 1. Monotonic and cyclic σ - ε curve.

$$\varepsilon = \frac{\sigma_{RO}}{E} + \left(\frac{\sigma_{RO}}{K'} \right)^{\left(\frac{1}{n'} \right)} \quad (1)$$

*Corresponding author. Tel.: ++421 41 513 2950, e-mail: milan.saga@fstroj.uniza.sk

The parameter E is Young's modulus, K is the cyclic strength coefficient, n is the cyclic strain-hardening exponent and σ_{RO} is the yield stress. All these material constants can be obtained from experimental dates or from Manson-Coffin curve parameters; this process will be presented latter.

The Wen's differential model in one of its possible modifications will be used for the further analysis. Its fundamental mathematic form is following [14,4]

$$z(z, x) = A \cdot \dot{x} - B \cdot |z|^{n-1} \cdot |\dot{x}| \cdot z - C \cdot |z|^n \cdot \dot{x} \quad (2)$$

The description of the material non-linearity can be formulated using so called Karray-Bouc model (KB) as a modification of Wen's model in the following form [14,4]

$$\begin{aligned} \sigma_{KB} &= \alpha \cdot E \cdot \varepsilon + (1 - \alpha) \cdot z \\ \dot{z} &= E \cdot \dot{\varepsilon} - \beta \cdot \frac{E}{R_e^n} \cdot |z|^{n-1} \cdot |\dot{\varepsilon}| \cdot z - \gamma \cdot \frac{E}{R_e^n} \cdot |z|^n \cdot \dot{\varepsilon} \end{aligned} \quad (3)$$

where $\alpha = E_T / E$ and z is the stress parameter. The other parameters written into the vector $\mathbf{p} = [\alpha, \beta, \gamma, n]^T$ influence the shape of the cyclic curve.

2. Calculation of RO model from Manson-Coffin curve and the identification of the KB model

2.1. Calculation of RO model parameters from Manson-Coffin curve

Let's consider the well-known Manson-Coffin curve

$$\varepsilon = \frac{\sigma'_f}{E} \cdot (2N)^b + \varepsilon'_f \cdot (2N)^c \quad (4)$$

where σ'_f is the fatigue strength coefficient, ε'_f is the fatigue ductility coefficient, b is the fatigue strength exponent, c is the fatigue ductility exponent. As mentioned in the introduction, these parameters can be used for the calculation of the Ramberg-Osgood model coefficients [5,9]:

$$n' = \frac{b}{c} \quad \text{and} \quad K' = \frac{\sigma'_f}{(\varepsilon'_f)^{n'}} = \frac{\sigma'_f}{(\varepsilon'_f)^{\frac{b}{c}}} \quad (5)$$

In the case of the steel STN 411373.0 the Manson-Coffin curve will be following

$$\varepsilon_{411373} = 0,003678 \cdot (2N)^{-0,078} + 0,371 \cdot (2N)^{-0,487} \quad (6)$$

and RO parameters can be calculated as follows

$$\begin{aligned} n'_{411373} &= \frac{b}{c} = \frac{-0,078}{-0,487} = 0,1602, \\ K'_{411373} &= \frac{\sigma'_f}{(\varepsilon'_f)^{n'}} = \frac{743}{0,351^{0,1602}} = 878,6. \end{aligned} \quad (7)$$

Tab.1 presents the results of our calculation for the chosen kinds of steels.

Steel STN	R _m [MPa]	R _e [MPa]	E [MPa]	ε' _f [-]	σ' _f [MPa]	b	C	K□ [MPa]	n□
411 373.0	414	299	202000	0,351	743	0,078	0,487	878,6	0,1602
411523.1	542	345	198000	0,871	1132	0,115	0,579	1163,5	0,1986
412 010.1	388	260	210600	0,326	699	0,098	0,492	873,8	0,1992
415 320.6	789	704	207000	0,936	1038	0,072	0,652	1045,0	0,1104

Tab. 1. Table of Manson-Coffin curve and RO model parameters.

2.2. Identification of the KB model

Assuming that the behaviour of monotonic curves σ-ε will be equivalent for both models RO and KB, the vector **p** can be obtained by a numerical approach using an optimising method implemented in Matlab. The objective function can be formulated [9] as follows

$$F(\mathbf{p}) = \int_0^{\varepsilon_{\max}} [\sigma_{KB}(\mathbf{p}) - \sigma_{RO}(K', n')] \cdot d\varepsilon \rightarrow \min \text{ or } F(\mathbf{p}) = \|\sigma_{KB}(\mathbf{p}) - \sigma_{RO}(K', n')\| \rightarrow \min. \quad (8)$$

where **p** = [α, β, γ, n]^T will be the vector of the optimised variables. The relationship σ_{KB}(**p**) - ε can be expressed as follows

$$\sigma_{KB}(\mathbf{p}) = \alpha \cdot 2,02 \cdot 10^{11} \cdot \varepsilon + (1 - \alpha) \cdot z(\mathbf{p}) \quad \text{where} \quad (9)$$

$$\dot{z}(\mathbf{p}) = 2,02 \cdot 10^{11} \cdot \dot{\varepsilon} - \beta \cdot \frac{2,02 \cdot 10^{11}}{(299 \cdot 10^6)^n} \cdot |z|^{(n-1)} \cdot |\dot{\varepsilon}| \cdot z - \gamma \cdot \frac{2,02 \cdot 10^{11}}{(299 \cdot 10^6)^n} \cdot |z|^n \cdot \dot{\varepsilon}$$

and σ_{RO}(K', n') - ε can be formulated as

$$\varepsilon = \frac{\sigma_{RO}}{2,02 \cdot 10^{11}} \quad \text{if} \quad \sigma_{RO} \leq 299 \cdot 10^6 \quad (10)$$

$$\varepsilon = \frac{\sigma_{RO}}{2,02 \cdot 10^{11}} + \left(\frac{\sigma_{RO}}{878,6 \cdot 10^6} \right)^{\left(\frac{1}{0,1602} \right)} \quad \text{if} \quad \sigma_{RO} > 299 \cdot 10^6.$$

Minimizing (8) the mathematical expression of the KB model describing material STN 411 353.0 for strain amplitude ε ∈ <0; 0,0282> the following expressions have been obtained

$$\sigma_{KB-411353} = 0,0246 \cdot 2,02 \cdot 10^{11} \cdot \varepsilon + (1 - 0,0246) \cdot z \quad \text{and} \quad (11)$$

$$\dot{z} = 2,02 \cdot 10^{11} \cdot \dot{\varepsilon} - 0,5710 \cdot \frac{2,02 \cdot 10^{11}}{(299 \cdot 10^6)^{0,4057}} \cdot |z|^{0,5943} \cdot |\dot{\varepsilon}| \cdot z - 0,3488 \cdot \frac{2,02 \cdot 10^{11}}{(299 \cdot 10^6)^{0,4057}} \cdot |z|^{0,4057} \cdot \dot{\varepsilon}$$

Fig. 2 shows the graphic representation of the identification process using Nelder-Mead optimising method for steel STN 411 373.0.

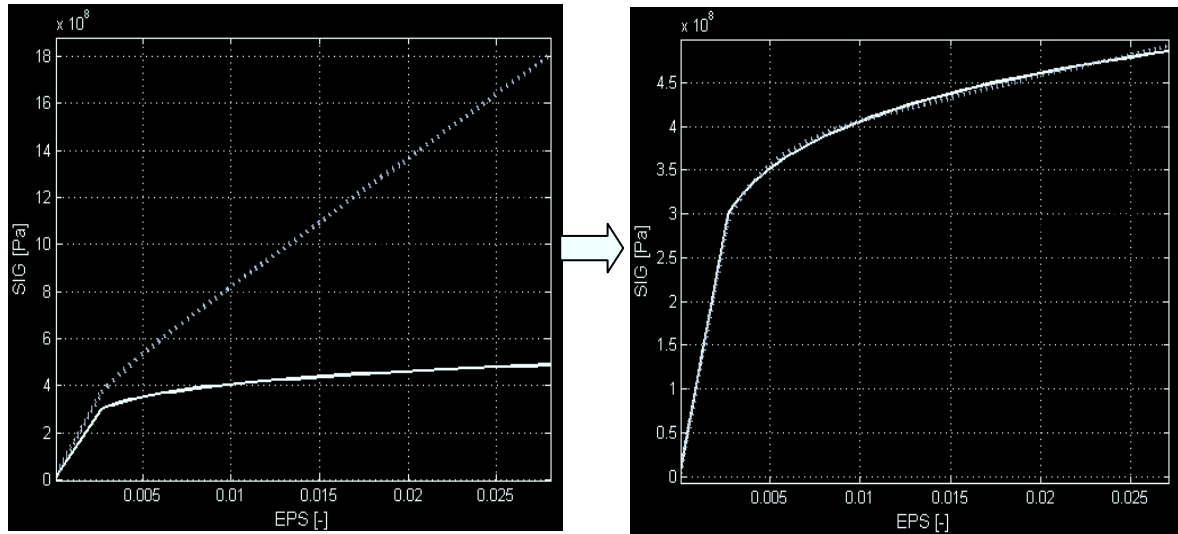


Fig. 2. Monotonic part σ - ε curve for material STN 411353.0 before and after the identification process.

Results of the identification process for other materials are presented in Tab.2. Using these coefficients we can propose a material computational model (KB, RO) for FEM or other analyses.

Using this numerical approach the KB computational model has been prepared for the hysteretic loop analysis (Fig. 3) and for the numerical calculation of the total strain-energy density per a cycle or the hysteretic energy per a cycle for different strain amplitudes.

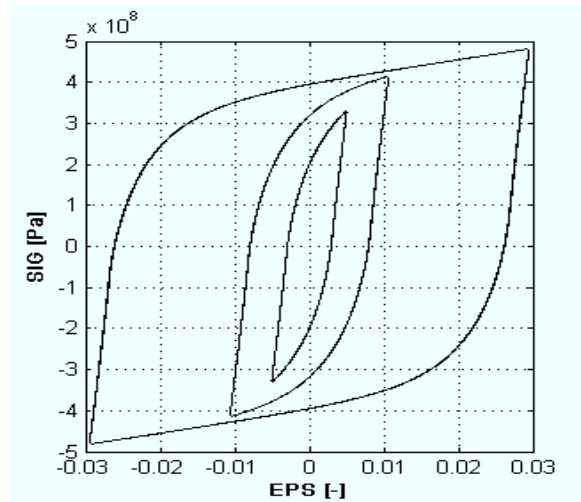


Fig. 3. σ - ε hysteretic loop (STN 411353) for amplitudes $\varepsilon_{\max} = 0,0282$ $\varepsilon_{\max} = 0,01065$ and $\varepsilon_{\max} = 0,00435$.

Steel	K□	n□	α	β	γ	n
11 373.0	878,6	0,1602	0,0139	0,3182	0,5935	0,3053
11523.1	1163,5	0,1986	0,0111	0,4123	0,5143	0,1915
12 010.1	873,8	0,1992	0,0150	0,7490	0,2034	0,1972
15 320.6	1045,0	0,1104	0,0083	0,5505	0,5336	1,2892

Tab. 2. Table of RO and KB material parameters.

3. Strain-energy density and hysteretic energy calculation

Considering the harmonic character of the strain amplitude $\varepsilon = \varepsilon_{\max} \cdot \sin(2\pi \cdot t)$, the eq. (11) will be solved for $t \in \langle 0, 10 \text{ sec.} \rangle$, $\varepsilon_{\max} \in \langle 0,00001 ; 0,028 \rangle$. By the obtained results it is possible to describe σ - ε hysteretic loop for the analysed material and a value of the stress ampli-

tude σ_{max} . Using the expression σ - ϵ in a discrete form the dissipative (hysteretic) energy density can be calculated [1,11] as follows

$$W_D = \int_{t_1}^{t_2} \sigma \cdot \dot{\epsilon} \cdot dt, \quad (12)$$

where t_1 is the time of the first stress maximum achievement and t_2 is the time of the second stress maximum achievement. In the case of the total strain energy density it is necessary to add the elastic part, i.e.

$$W_E = \frac{\sigma_{max}^2}{2 \cdot E}. \quad (13)$$

A calculation of the total strain energy density per half cycle can be realised using a well-known Feltner's term [13]

$$W_F = \sigma_{max} \cdot \epsilon_{max p} \cdot \frac{2}{1+n'} + \frac{\sigma_{max}^2}{2 \cdot E} \quad (14)$$

and for the hysteretic energy density per cycle the Morrow's relationship is often applied [13],

$$W_M = 4 \cdot \sigma_{max} \cdot \epsilon_{max p} \cdot \frac{1-n'}{1+n'}. \quad (15)$$

It's important to note that these relationships are approximate, very simple, what is their facility. Our proposed numerical approach is more complicated but much more accurate. Of course, the relation σ - ϵ cannot be solved explicitly.

4. Energy-based fatigue curve

Applying the KB computational model, the energy-based fatigue curve will be obtained from Manson-Coffin curve (4). Using (14) or (15) it's possible to express the analysed curve in an explicit form, mainly from the comparison point of view. The Feltner's explicit expression is following [13]

$$W_F = \sigma_f' \cdot (2N)^b \cdot \left[\frac{2}{1+n'} \cdot \epsilon_f' \cdot (2N_f)^c + \frac{\sigma_f'}{E} \cdot (2N_f)^b \right]. \quad (16)$$

This expression can be applied for both the low and the high cycle fatigue analysis. Morrow's energy fatigue curve is applicable for the low cycle first of all. Its mathematical notation is known in the following form [13]

$$W_M = 4 \cdot \frac{1-n'}{1+n'} \cdot \sigma_f' \cdot \epsilon_f' \cdot (2N)^{b+c}. \quad (17)$$

On the basis of the proposed ideas it's possible to present the fatigue curves for steel STN 411353.0 in several modifications. Next figures show:

- the classic Manson-Coffin curve (Fig.4),
- the energy fatigue curve obtained by the numerical computation (Fig.5),
- the comparison of the energy fatigue curve obtained by the numerical computation and by Feltner's expressions (Fig.6) and finally
- the comparison of the energy fatigue curve obtained by the numerical computation and by Morrow's expressions (Fig.7).

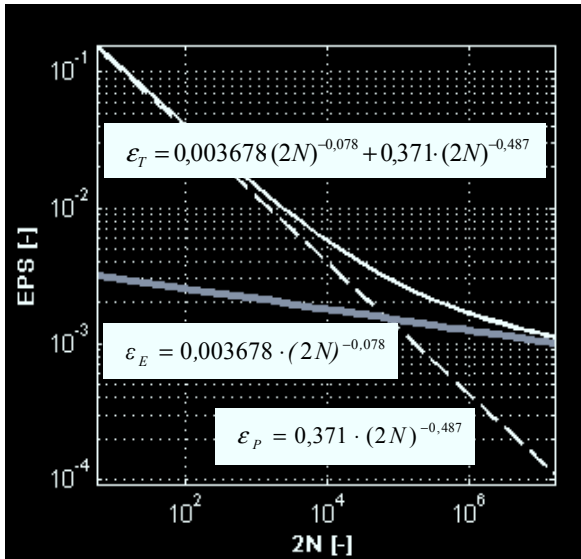


Fig. 4. ϵ -2N fatigue curve.
Steel STN 411353.0.

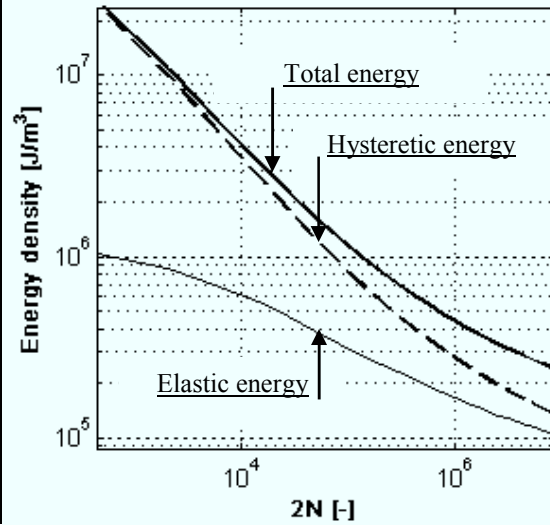


Fig. 5. Energy fatigue curve.
Strain-energy density per a cycle
vs. the number of the reversals.

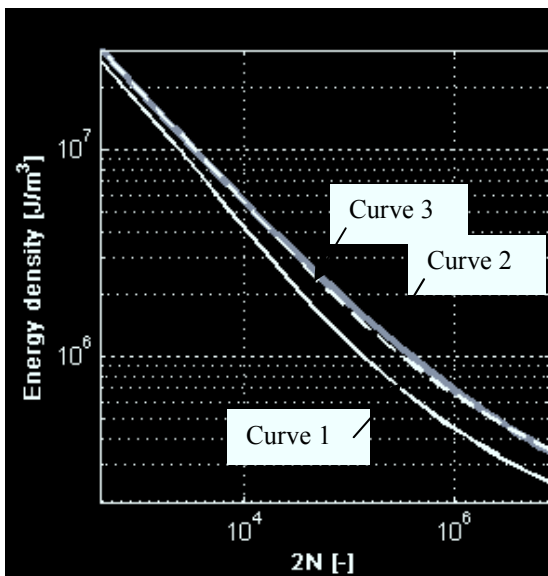


Fig.6. Energy fatigue curve.
Strain-energy density per a cycle
vs. the number of the reversals.
Curve 1: presented calculation
Curve 2: Feltner's calculation (14)
Curve 3: Feltner's calculation (16)

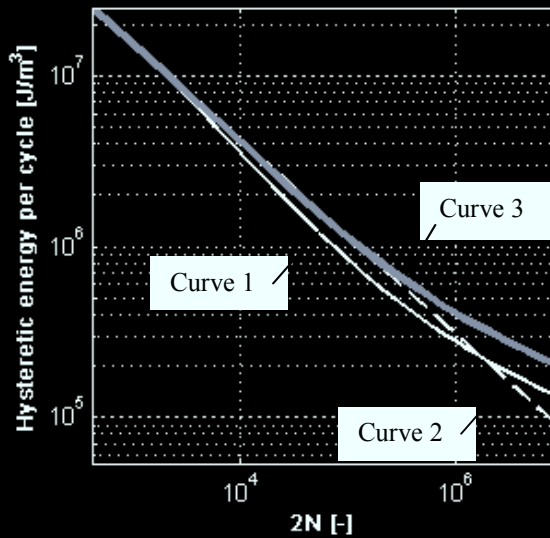


Fig.7. Energy fatigue curve.
Strain-energy density per a cycle
vs. the number of reversals.
Curve 1: presented calculation
Curve 2: Morrow's calculation (15)
Curve 3: Morrow's calculation (17)

Considering the strain energy density as the fatigue parameter the proposed solution can be very problematic, because it is not possible to determine the loading type from history of the energy $W(t)$. This problem is typical for the case of the rainflow analysis. In [7,8] the authors defined $W(t)$ taking into account the signs of stresses and strains in order to distinguish the energy under the tension (+) and under the compression (-) as follows

$$W_1(t) = \frac{1}{2} \cdot \sigma(t) \cdot \epsilon(t) \cdot \frac{\text{sign}(\sigma) + \text{sign}(\epsilon)}{2}. \quad (18)$$

For distinguishing between the positive and negative parameter of an strain energy density, the function *sign* has been introduced into the elastic energy density expression [7,8]. Another computational approach considering the "positive" and "negative" character of the strain energy density may be defined (from author's experience) as follows

$$W_2(t) = \frac{1}{2} \cdot \sigma(t) \cdot \varepsilon(t) \cdot \text{sign}(\varepsilon). \tag{19}$$

Character of the expressions (18), (19) and their comparison with strain behaviour is shown on Fig. (8). Energy-based fatigue life estimation can be used for multiaxial loading settings mainly in the cases of the non-proportional conditions [1].

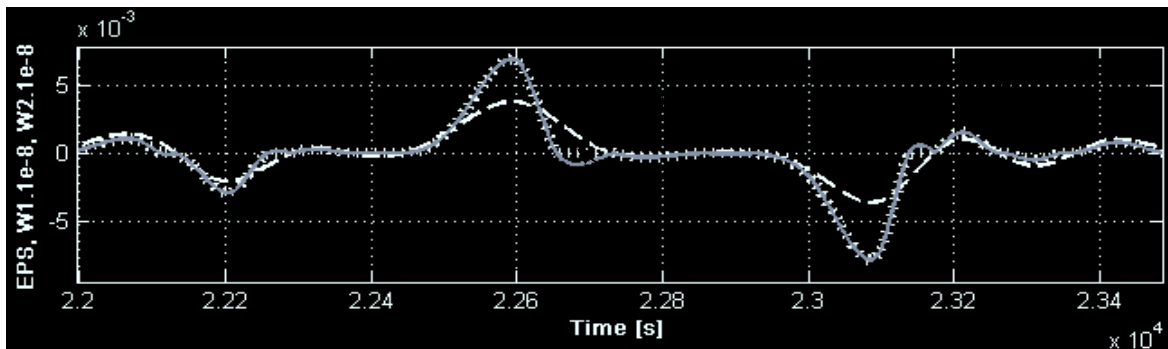


Fig. 8. Comparison of the relations $\varepsilon(t)$, $W_1(t)$ and $W_2(t)$.

Proposed computational techniques can be compared in following simple example. Let's consider a random behaviour of $\varepsilon(t)$. By (18), (19) we can calculate the "positive" or "negative" energy density $W_1(t)$ or $W_2(t)$ and also the rainflow analysis apply. A cumulative damage D is assumed as a comparative parameter. Finally, it's compared the "classic" Manson-Coffin damage calculation with "energy" damage calculation using $W_1(t)$ and $W_2(t)$. Results of this short study are presented in Tab.3.

Manson-Coffin cumulative damage	W ₁ calculation technique			W ₂ calculation technique		
	Feltner	Morrow	Presented method	Feltner	Morrow	Presented method
0,093	0,86	0,089	0,091	0,087	0,092	0,094

Tab. 3. Table of the cumulative damage D.

5. Conclusion

The goal of this paper was to present the chosen computational tools for an energy-based fatigue life estimation. A numeric approach for an identification of the hysteretic Karray-Bouc material model from Ramberg-Osgood model parameters, which have been calculated from Manson-Coffin curve, has been proposed. Using Karray-Bouc model the energy fatigue curve has been obtained and consequently compared with Feltner's and Morrow's curves. Results shown in figures 6 and 7 indicate that the energy fatigue curves behaviours are a bit different. It leads to a claim that the energy fatigue life prediction using Feltner's or Morrow's methods can give a slightly garbled information. However, the numerical tests using rainflow decomposition indicate feasible values of the damage.

Acknowledgement

The work has been supported by the grant project VEGA1/3168/06 and KEGA3/5028/07.

References

- [1] M. Balda: A New Method for Fatigue Life Estimation using the Stochastic Load, *Computational Mechanics 2006*, Volume 1, Nečtiny, str. 57-62.
- [2] M. Balda, J. Svoboda: Energetic Criteria Application for the Construction Life Computation under the Multiaxial Stochastic Disproportional Load, *Computational Mechanics 2003*, Nečtiny, 2003, str. 23-28.
- [3] V. Deký, A. Sapietová, R. Kocúr: On the reliability estimation of the conveyer mechanism using the Monte Carlo method, *Proc. COSIM2006*, Krynica-Zdroj, 2006, pp.67-74.
- [4] R. H. Cherng, Y. K. Wen: Stochastic finite element analysis of non-linear plane trusses. *Int. J. Non-Linear Mechanics*, Vol. 26, No. 6, 1991, pp. 835-849.
- [5] M. Klesnil a kol.: *Cyclical Deformation and Metal Fatigue*, VEDA/vydavateľstvo Slovenskej akadémie vied Bratislava, 1987.
- [6] V. Kliman: Fatigue Life Estimation for the Loading Process Stochastic Procedure, *Strojnícky časopis*, 36, 1985, č.4-5, str. 519-530.
- [7] T. Lagoda, E. Macha: Energy approach to fatigue life estimation under combined tension with torsion, *Zeszyty Naukowe Politechniki Opolskiej*, Nr.kol.269/2001, pp.163-182
- [8] E. Macha, C. M. Sonsino: Energy criteria of multiaxial fatigue failure, *Fatigue Fract. Engng Mater. Struct.*, Vol 22, 2000, pp.1053-1070
- [9] J. Mazúr, V. Deký, R. Melicher: Optimization Method Application for the Material Characteristics Identification, *Acta Mechanica Slovaca*, 4-B/2006, str. 229-238.
- [10] V. V. Ogarevic, J. Aldred: An implementation of low-cycle multiaxial fatigue methods, *ECCM-2001*, European Conference on Computational Mechanics, June 2001, Cracow, Poland.
- [11] W. F. Pan, Ch. Y. Hung, L. L. Chen: Fatigue life estimation under multiaxial loadings, *Int. J. of Fatigue*, Vol. 21, 1999, pp. 3-10.
- [12] J. Papuga, M. Růžicka: Uniaxial and Multiaxial Methods for the Life Solution from the Algorithmization Perspective, *Computational Mechanics 2001*, Nečtiny 2001, str. 269-278.
- [13] M. Růžicka, M. Hanke, M. Rost: *Dynamical Stiffness and Lifetime*, ČVUT Praha, 1989.
- [14] M. Sága: Numerical Study of the Nonlinear Truss Structures Stochastic Vibration, *Strojnícky časopis*, Vol. 52, No. 4, 2001, str. 208-220.
- [15] F. Trebuňa, F. Šimčák: *Mechanical System Elements Resistance*, Technická univerzita v Košiciach, Košice 2004, ISBN 80-8073-148-9.